Metal−Olefin Bond Energies in $M(CO)_5(C_2H_{4-n}Cl_n)$ M = Cr, Mo, W; $n = 0-4$: Electron-Withdrawing Olefins Do Not Increase the Bond Strength

Darin N. Schlappi and David L. Cedeño*

Department of Chemistry, Illinois State University, Box 4160, Normal, Illinois 61790-4160

Received: March 26, 2009; Revised Manuscript Received: July 17, 2009

Metal−olefin bond dissociation enthalpies have been calculated for the series of complexes $M(CO)_5(C_2H_{4-n}Cl_n)$, M = Cr, Mo, W; $n = 0-4$ using density functional theory. Experimental values of the bond enthalpies have been measured for $M(CO)_5(C_2H_{4-n}Cl_n)$ M = Cr, Mo, W; $n = 2$ (vinyl chloride), 3, and 4 using laser photoacoustic calorimetry in n-hexane solution. Experimental and calculated values indicate that the trend in metal−olefin bond energies is opposite to the electron-withdrawing ability of the olefin, which is counter to expectations based on the Dewar−Chatt−Duncanson model for metal−olefin bonding. An in-depth analysis of the metal−olefin interaction using a bond energy decomposition scheme implies that the observed and calculated decreasing trend is influenced by the increase in steric interactions and olefin reorganizational energy which is concomitant to the increase of the number of electron-withdrawing halogen atoms.

Introduction

Many significant chemical processes such as olefin hydrogenation, isomerization, hydrocarbonlyation, hydroformylation, polymerization, and metathesis among others are driven by the presence of a metal catalyst and involve the formation of an intermediate that contains a metal−olefin bond.[1−6] It is beneficial to be able to synthesize catalysts for these reactions that are fine-tuned to the needs of a particular reaction or process because the use of olefins and olefin-related products in industry has become prevalent. The ability to control the properties of these catalysts relies heavily on a complete understanding of the thermodynamic factors that influence the strength of the bond between a given metal complex and an olefin.

Contributing to a level of understanding that would allow for an accurate prediction of the bond strength between a metal complex and an olefin is the primary goal of our research. The current picture of metal−olefin bonding is based on frontier molecular orbital theory introduced by Dewar in 1951[7] and expanded by Chatt and Duncanson in 1953.[8] The approach is known as the Dewar−Chatt−Duncanson (DCD) model of metal−olefin bonding. The DCD model details the metal−olefin bond as being a two way synergistic electron exchange between a metal complex and an olefin. The bond consists of a σ interaction in which the highest occupied molecular orbital (HOMO) of the olefin donates electron density to an empty d_σ orbital on the metal complex. Additionally, there is a π bonding interaction in which the metal donates electron density back to the olefin from an occupied d_π orbital to the unoccupied antibonding π^* orbital of the olefin.

The electron population changes in the π and π^* orbitals of the olefin have the physical consequence of decreasing the bond order of the carbon−carbon double bond. This is equivalent to a partial sp^2 to sp^3 rehybridization of the olefinic carbons that causes the lengthening of the C=C bond and the back-bending of the substituents around the C=C bond away from the metal complex and outside of the plane of the C=C bond. The DCD model has been commonly used to rationalize the bonding strength between a metal complex and an olefin.[2,5,9] A widespread expectation of this rationalization is that for some metals the π (or back-) bonding interaction is the dominating contribution to the metal−olefin bond. Therefore, if the hydrogen atoms in ethylene were to be replaced with a more electron-withdrawing substituent such as a halogen (X = F, Cl), then the back-bonding would increase because a halogenated ethylene is a better π acceptor than ethylene. Based on this rationalization, the bonding energies between a metal and the olefin series C_2H_4, C_2F_4, and C_2Cl_4 would be a function of the electron-withdrawing ability of the substituents around the C=C bond of the olefin and decrease in the order $C_2F_4 > C_2Cl_4 > C_2H_4$. Experimental data on $Cr(CO)_5(C_2X_4)$ (where X = H, F, Cl) indicate, however, that the metal−olefin bond strength follows the trend $Cr-C_2H_4 > Cr-C_2F_4 > Cr-C_2Cl_4$.[10] Cedeño and Weitz[10] carried out a Density Functional Theory (DFT) study of the series $Fe(CO)_4(C_2X_4)$ and $Cr(CO)_5(C_2X_4)$ where X = H, F, Cl, that provides an explanation for the discrepancy between the experimental data and the expectations based on the DCD model.

Along the same line of reasoning, the DCD model may be used to predict the trend of the metal bond strength for the olefin series $C_2H_{4-n}X_n$ (X = F or Cl). Given that the back-bonding ability of an olefin is enhanced as halogenation increases, then the metal−olefin bond strength should increase with an increase in the number of halogens. Back in 1974, Tolman[11] determined the equilibrium bonding constants between bis(tri-*o*-tolyl phosphite)nickel(0) and 38 different olefins including the $C_2H_{4-n}F_n$ ($n = 0-4$) series. In his paper, Tolman found that none of the fluoro olefins examined (with the exception of $CH_2{=}CHCF_3$) were as good as C_2H_4 in coordinating to nickel(0), a surprising result that was out of line with his expectation. Tolman hinted that the reason for the inadequacy of the DCD picture of metal−olefin bonding was due to the reorganization that occurs in the olefin as the carbons of the double bond are forced to rehybridize from sp^2 to sp^3. A computational DFT study by Schlappi and Cedeño[12] examined the bonding of the olefins $C_2X_nH_{4-n}$ (X = F or Cl, and $n = 0-4$) to $Ni(PH_3)_2(CO)$. It was found that the olefins bound to the nickel with dissociation energies that follow a trend very similar to the one shown in Tolman's study and confirmed his presumption. We concluded

---

* Corresponding author. Email: dcedeno@ilstu.edu.

10.1021/jp9027468 CCC: \$40.75

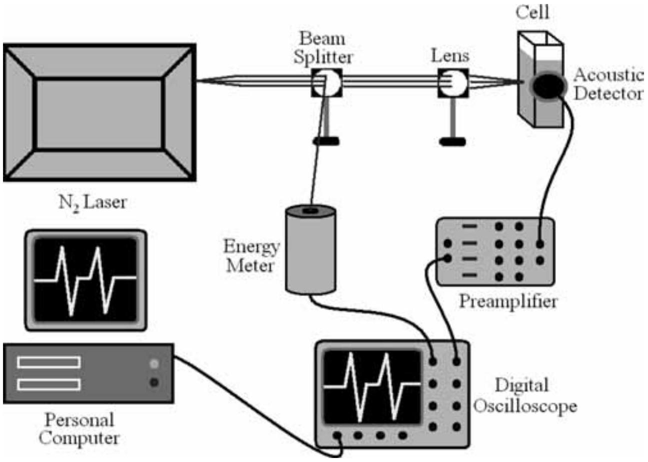

Figure 1. A representation of the experimental setup used for LPAC.

that there is an energetic cost of the reorganization of not only the olefin but the metal fragment as well. This energetic cost must be overcome as the metal binds to the olefin and is accountable for the discrepancy between the DCD picture and experimental results. In addition, steric repulsion is also a factor, especially when the olefin contains bulky substituents around the double bond. These studies indicate that the DCD model may be an accurate portrayal of the molecular orbital interactions that occur between a metal and an olefin, but it is not a complete description of all of the factors that influence the strength of the metal and olefin bond.

In this manuscript we present experimental bond strengths obtained using laser photoacoustic calorimetry (LPAC) along with DFT calculations that are utilized to investigate the bonding between olefin and metal in the complex series $M(CO)_5(C_2H_{4-n}Cl_n)$ where M is Cr, Mo, or W and $n = 0-4$. This olefin series provides a steady increase in electron-withdrawing capability of the olefin as the hydrogen atoms around ethylene are replaced with chlorine. LPAC provides bond dissociation enthalpies, which serve as a measurement of bond strength. The DFT studies complement LPAC experiments by providing an in depth analysis of the factors that influence the metal−olefin bond. DFT has been shown to be a powerful tool for determining properties of many electron systems that are difficult using experiments, and it allows for the fairly accurate calculation of bond energies.[13−17] A bond energy decomposition analysis is carried out that breaks down the bond dissociation energy of a metal and olefin into its component contributions. The changes that occur in all of these components were compared in relation to one another and in terms of their contribution to the total bond energy. In addition, the changes that occur to geometry and energy contributions, as well as electron populations, were tracked based on the number of chlorines present and the identity of the metal in the metal fragment.

Experimental and Computational Methods

Laser Photoacoustic Calorimetry. Experimental bond dissociation enthalpies were obtained using laser photoacoustic calorimetry (LPAC).[18,19] The LPAC setup is shown in Figure 1. Bond enthalpies were determined for the series $M(CO)_5$-$(C_2H_{4-n}Cl_n)$ with M = Cr, Mo, or W and $n = 2$ (1,1-dichloroethene), 3, or 4. Metal hexacarbonyls were obtained from Strem Chemicals; the olefins and solvent (n-hexane) were obtained from Acros Organics and dried using molecular sieves. Argon-purged hexane solutions containing 0.3 or 0.4 M of the chlorinated olefin (C_2Cl_4, C_2HCl_3, or iso-$C_2H_2Cl_2$) and 0.1 mM of either chromium, molybdenum, or tungsten hexacarbonyl were placed in a 1 cm cuvette. A nitrogen laser (PTI, GL-3300, $\lambda = 337$ nm, 1.5 mJ/pulse) was used to induce the formation of the metal−olefin complex via dissociation of a metal−carbonyl bond. A beam splitter sent a portion of the laser beam to a pyroelectric energy meter (PTI, L-PEDm, 2 mV/μJ) used to track the pulse energy. The remaining beam was sent through a focusing lens and an iris to control the width of the laser beam hitting the sample. The beam diameter at the sample cuvette is about 1−2 mm.

The photoacoustic wave generated as a result of the heat released by the chemical system exposed to the laser was detected using a piezoelectric ultrasonic pressure transducer (Panametrics A103s, 1 MHz). The signal from the detector was amplified (×50, Panametrics 5662) and sent to a digital storage oscilloscope (LeCroy 9314CM, 400 MHz). A silicon photodiode was used as an optical trigger for data acquisition. Signals from the energy meter and ultrasonic transducer were acquired simultaneously and averaged over 40 laser pulses. A solution of ferrocene in n-hexane was used as calorimetric reference.[19] Absorbances of all solutions at 337 nm were measured before and after each calorimetric determination using a Thermo Spectronic Genesys spectrophotometer and fell within a range of 0.100 to 0.175 absorbance units. The absorbances of the sample and reference at 337 nm were matched within a 0.005 absorbance units. Photoacoustic signals for the reference and sample were transferred from the oscilloscope to a personal computer for analysis with commercial sound analysis software.[20] Bond dissociation enthalpies are obtained from the average of at least five runs for each sample and reference solution pair.

Geometry Optimizations. Geometries and energies for all molecular structures were calculated using density functional theory (DFT) with the ADF2008 quantum chemistry program.[21] All calculations were carried out using the BP86 functional. BP86 is a gradient-corrected functional that uses Becke's 1988[22] functional for exchange, and Perdew's 1986[23,24] and Vosko, Wilk, and Nusair's (VWN) functionals[25] for correlation. The basis set utilized is a relativistic zero order regular approximation (ZORA) STO-TZP available in the ADF program.[26−28] The (ZORA) STO-TZP is a triple-ζ basis set that also employs a polarization function for all atoms.

Bond Energy Calculations. Gas phase metal−olefin bond energies (ΔE) were obtained for the following reaction using the calculated energies of the optimized ground-state geometries:

$$M(CO)_5(C_2H_{4-n}Cl_n) \rightarrow M(CO)_5 + C_2H_{4-n}Cl_n \quad (1)$$

For which:

$$\Delta E = E[M(CO)_5] + E[(C_2H_{4-n}Cl_n)] - E[M(CO)_5(C_2H_{4-n}Cl_n)] \quad (2)$$

As written, eq 1 is a dissociation reaction; thus, all reported ΔE represent bond dissociation energies and are positive. We have adopted, throughout this work, a convention in which factors favorable for bonding are positive and those unfavorable for bonding will be negative. Calculated bond enthalpies (ΔH_{298}) at 298 K were obtained using the following equation:

$$\Delta H_{298} = \Delta E + \Delta ZPE + \Delta E_{th} + \Delta(PV) \quad (3)$$

ΔZPE is the zero point energy difference, ΔE_{th} is the change in thermal energy for rotations, vibrations, and translations in going from 0 to 298 K, and $\Delta(PV)$ is the molar work. Zero point energies and thermal corrections were obtained from analytical frequency calculations using the Jaguar computational program and the same DFT functional.[29] The LACV3P** basis set available in Jaguar was used. This basis set reproduces very well the geometries and energies obtained using ADF. The LACV3P** utilizes relativistic Hay and Wadt's Effective Core Potentials (ECP)[30] and the 6-31G basis set to describe metal atoms, and the 6-311G** basis set to describe nonmetals.[31−34]

Bond Energy Decomposition Analysis. Bond energies were further broken down using the Bond Energy Decomposition Analysis (BEDA) scheme[35,36] implemented in the Amsterdam Density Functional program (ADF04).[21] The analysis carries out a BP86 single point energy calculation on optimized structures in order to break the bond dissociation energy into contributions from four different terms:

$$\Delta E = \Delta E_{oi} + \Delta E_{elect} + \Delta E_{Pauli} + \Delta E_{reorg} \tag{4}$$

ΔE_{oi} is the orbital interaction energy, which is an attractive contribution from the interactions of occupied orbitals of one reactant from eq 1 with the unoccupied orbitals of the other reactant. This term also accounts for interactions between unoccupied and occupied orbitals within the same reactant. ΔE_{elect} is the electrostatic interaction energy, which results from Coulombic attractive interactions between the two reactants. ΔE_{Pauli} is the Pauli repulsion energy due to the repulsion between the occupied orbitals of the two reactants. ΔE_{reorg} is the reorganizational energy, which represents the energy involved in deforming the geometries of the reactants in their ground states to the geometries they adopt in the final complex. The reorganizational energy may be further decomposed as:

$$\Delta E_{reorg} = \Delta E_{reorg}(\text{olefin}) + \Delta E_{reorg}(\text{M(CO)}_5) \tag{5}$$

The two terms in this equation account for the geometry changes that must occur in the free olefin and the metal pentacarbonyl during bonding. The sum of the first three terms in eq 4 is referred as the interaction energy (ΔE_{int}):

$$\Delta E_{int} = \Delta E_{oi} + \Delta E_{elect} + \Delta E_{Pauli} \tag{6}$$

This interaction energy is simply the net bonding interaction that would occur between two reactants once they have reorganized into the conformations that would be found in the bound complex.

Results

Experimental Bond Enthalpies. Laser photoacoustic calorimetry (LPAC) has been shown to be a reliable method for the determination of solution-phase bond enthalpies in transition metal compounds.[37−42] The heat released from the reacting system results in a pressure wave that is detected using a pressure transducer coupled to the wall of the container. The amplitude of the wave is proportional to the heat emitted via the parameter ϕ which is the fraction of absorbed laser energy released as heat. The use of a suitable calorimetric reference (one for which $\phi = 1$) allows for the calibration of the instrument. The analysis of the calorimetric data is based on the fact that the photoinduced formation of the olefin complex in n-hexane solution involves the following two-step process:[39]

$$\text{M(CO)}_6 + \text{solvent} + \text{light} \rightarrow \text{M(CO)}_5(\text{solvent}) + \text{CO} \tag{7}$$

$$\text{M(CO)}_5(\text{solvent}) + \text{olefin} \rightarrow \text{M(CO)}_5(\text{olefin}) + \text{solvent} \tag{8}$$

The conditions of the system are adjusted such that these steps occur on different time scales. The first process occurs in a time scale that is faster than the temporal resolution of the transducer (about 5 ns). The time scale of the second step depends on the concentration of olefin, which is adjusted in such a way that the process occurs in a time scale between 50 and 2000 ns. Deconvolution of the acoustic signal of the sample relative to that of the reference allows the iterative calculation of two sets of ϕ and τ (lifetimes) values, that correspond to the emission of heat during the two steps (eqs 7 and 8). From the energy balance it is possible to obtain the enthalpy for reactions 9 and 10 according to:[39]

$$\Delta H_1 = \left(\frac{(1 - \varphi_1)E_{h\nu}}{\Phi_{\text{reaction}}} + \frac{\Delta V_1}{\chi}\right) \tag{9}$$

$$\Delta H_2 = \left(\frac{-\varphi_2 E_{h\nu}}{\Phi_{reaction}} + \frac{\Delta V_2}{\chi}\right) \tag{10}$$

In eqs 9 and 10, E_{hv} is the molar photon energy, Φ_{reaction} is the reaction quantum yield, ΔV is the reaction volume change, and χ is the solvent expansivity. Utilization of eq 9 allows the determination of metal−solvent bond enthalpies if the metal−CO bond enthalpy is known. Previous work by Burkey and co-workers[37,39] have determined metal−solvent bond energies that rely on the quantification of ΔH_1 and ΔV_1. Analogously, the utilization of eq 10 allows the determination of a metal−olefin bond enthalpy if the metal−solvent bond enthalpy is known, once ΔH_2 and ΔV_2 are determined. Since this is the focus of this work, we only report values obtained upon utilizing eq 10 neglecting the volume change (ΔV_2). Burkey and co-workers report a small volume change (<1 mL/mol) for the displacement of a linear alkane by tetrahydrofuran.[39] Given that the halogenated ligands have molecular volumes similar to that of tetrahydrofuran, we expect volume changes of the same magnitude. In such case neglecting the effect of the volume change will carry out a variation within the range of the experimental uncertainties.

Table 1 shows experimental parameters (ϕ_1, τ_1, ϕ_2, and τ_2) obtained for the M(CO)$_5$(olefin) complexes, where M = Cr, Mo, W and olefins = C_2Cl_4, C_2HCl_3, and iso-$C_2H_2Cl_2$ (1,1-dichloroethene). It is worth mentioning that τ_1 does not represent the actual time scale of the formation of the solvento complex, which is expected to occur much faster; instead it represents the temporal resolution of the transducer (~5 ns). The enthalpy (ΔH_2) of the solvent displacement reaction (eq 9) was then calculated according to eq 10 assuming a negligible volume change. The molar photon energy of the laser pulse is equal to 84.9 kcal/mol, while the reaction quantum yield is taken to be 0.70 based on reported values for similar reactions.[37] The enthalpies for bond dissociation of the olefin from the M(CO)$_5$ were estimated using the fact that ΔH_2 is equal to the difference

TABLE 1: Experimental Values of ϕ_1, τ_1, ϕ_2, and τ_2 and Bond Energetics from LPAC[a]

bond	ϕ_1	τ_1 (ns)	ϕ_2	τ_2 (ns)	ΔH_2	ΔH_{LPAC}[b]
Cr−C_2Cl_4	0.82 ± 0.03	4.8 ± 0.8	0.034 ± 0.027	1210 ± 930	−4.1 ± 2.2	13.5
Cr−C_2HCl_3	0.81 ± 0.05	4.3 ± 0.7	0.035 ± 0.004	1180 ± 490	−4.2 ± 0.5	13.7
Cr-iso$C_2H_2Cl_2$	0.766 ± 0.002	3.6 ± 2.2	0.040 ± 0.008	910 ± 360	−4.9 ± 1.0	14.3
Mo−C_2Cl_4	0.775 ± 0.025	4.7 ± 1.4	0.047 ± 0.007	550 ± 130	−5.7 ± 0.8	11.4
Mo−C_2HCl_3	0.790 ± 0.021	0.8 ± 1.5	0.058 ± 0.010	690 ± 80	−7.0 ± 1.2	12.7
Mo-iso$C_2H_2Cl_2$	0.740 ± 0.008	3.8 ± 3.4	0.078 ± 0.016	1680 ± 710	−9.4 ± 1.9	15.1
W−C_2Cl_4	0.77 ± 0.04	5.6 ± 2.7	0.040 ± 0.006	270 ± 50	−4.9 ± 0.8	18.5
W−C_2HCl_3	0.762 ± 0.015	4.1 ± 3.5	0.063 ± 0.017	198 ± 25	−7.6 ± 2.0	21.1
W-iso$C_2H_2Cl_2$	0.774 ± 0.028	5.8 ± 6.6	0.071 ± 0.003	200 ± 8	−8.6 ± 0.3	22.2

[a] Enthalpies in kcal/mol. [b] ΔH_{LPAC} = BDE(M−solvent) − ΔH_2.

CHART 1

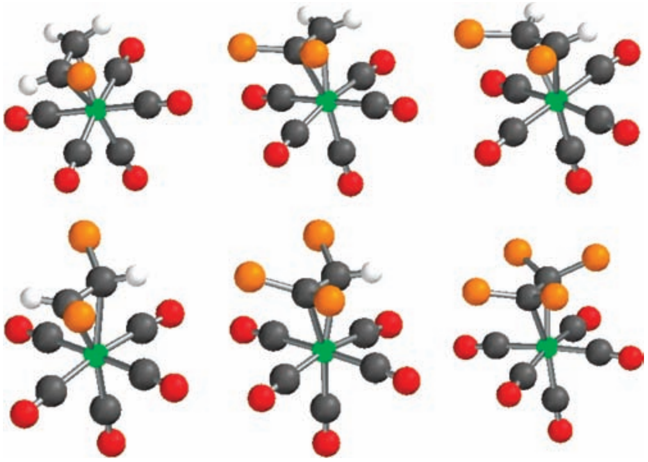

between the metal−olefin bond energy and the metal−solvent bond energy. Metal−solvent bond energies were obtained from the literature.[37,39,43] The experimental values of ΔH_2 and bond dissociation enthalpies (ΔH_{LPAC}) are given in Table 1. A previous gas-phase determination of the Cr−C_2Cl_4 bond enthalpy in $Cr(CO)_5(C_2Cl_4)$ of 12.6 kcal/mol is in good agreement with the 13.5 kcal/mol reported here for n-hexane solution.

Density Functional Theory (DFT) Geometry Optimizations. DFT geometry optimizations were performed for all molecules. To our knowledge there are no structural experimental data for the series $M(CO)_5(C_2Cl_nH_{4-n})$ (M = Cr, Mo, W; n = 1−4), but previous work on iron and chromium compounds have shown good structural agreement between DFT calculations and experimental data.[44,45] Typical structures of the molecules along with selected geometric parameters are shown in Chart 1 and Table 2.

All unbound olefins are planar, and the C═C bond distance varies with the number of chlorine substituents. The $M(CO)_5$ are square pyramidal in shape with the two sets of trans CO ligands roughly 180° opposite each other. Upon binding to an olefin, the C═C double bond of the olefin is parallel to one set of equatorial carbonyl groups, forcing these equatorial carbonyls of the $M(CO)_5$ complex to bend back away from the olefin. The flexing is accounted for in the C−M−C angle and represents the largest geometrical change in the unbound $M(CO)_5$ relative to the $M(CO)_5$ complex. As expected, the geometry of the olefin is changed upon binding. The substituents around the double bond bend away from the $M(CO)_5$ fragment as accounted for in the pyramidalization angle Θ (180 degrees minus the dihedral angle between trans substituents). Finally, as the bond is formed, the double bond of the olefin increases in length relative to its unbound state. Table 2 shows the most relevant calculated geometrical parameters.

DFT Bond Energies and Bond Energy Decomposition Analysis. Calculated bond energies and enthalpies for the dissociation of $M(CO)_5(C_2Cl_nH_{4-n})$ (M = Cr, Mo, W; n = 0−4) are shown in Table 3. Bond energies and enthalpies exhibit the same trends; for instance, ethylene makes the strongest bond to $M(CO)_5$, while C_2Cl_4 has the weakest bond. The calculated bond enthalpies are in good agreement with the experimental values (ΔH_{LPAC}, Table 1), taking into consideration that calculated DFT/BP86 values may be overestimated.[46] Table 4 shows the results of the BEDA according to eqs 5 and 6.

Discussion

Metal−Olefin Bond Energies. In general, the calculated bond enthalpies (Table 3) and trends are in good agreement with the experimental values (Table 1). It is important to note that the agreement is better for the tetrachlorinated olefin complexes (within 1 kcal/mol) while is poorer for the iso-dichlorinated olefin complexes (within 5 kcal/mol). Both experimental errors such as the neglect of volume changes and computational errors inherent to the incompleteness of basis sets and DFT functional are responsible for the differences. The calculations indicate that metal−olefin bond energies in the chromium and molybdenum compounds should be similar while the tungsten−olefin bond energies should be larger.

In all the results, one trend is obvious: As the number of chlorines around the double bond increases, the strength of the metal olefin bonds decreases. On the basis of the Dewar−Chatt−Duncanson model, an increase in the number of chlorines atoms around the double bond of an olefin should increase its electron-withdrawing ability, leading to an increase in back-bonding and a stronger bond between the metal and the olefin.[2] Thus, the results indicate that this anticipated trend is not observed. In fact, these indicate that the opposite occurs. Clearly, the magnitude of the metal−olefin bond energy is dependent on more than just orbital interactions in which the DCD model is solely based.

Metal−Olefin Bonding from a Molecular Orbital Perspective: The DCD Model Interpretation. As mentioned in the Introduction, the DCD model provides a qualitative frontier molecular orbital description of the metal−olefin bonding interactions. We have carried out a molecular orbital (MO) analysis in order to describe such interactions quantitatively in terms of the DCD model implications. The MO analysis provides a view of frontier MO energies, overlaps, and electron populations in both the $M(CO)_5$ portion of the complex and the olefin. Figure 2 shows calculated energy gaps, orbital overlaps, and changes in electron populations for the frontier MOs involved in the σ and π interactions between the $W(CO)_5$ complex and the olefin (similar plots for $Cr(CO)_5$ and $Mo(CO)_5$ are available as Supporting Information).

TABLE 2: Selected Calculated Geometrical Parameters for $M(CO)_5(C_2H_{4-n}Cl_n)$[a]

complex	$M-C_{olef}$	C=C	OC−M−CO	Θ^b (HC=CH)	Θ^b (HC=CCl)	Θ^b (ClC=CCl)
$Cr(CO)_5(C_2H_4)$	2.341	1.382	173.5	20.7	—	—
$Cr(CO)_5(C_2H_3Cl)$	2.316 (CH_2), 2.348 (CHCl)	1.382	172.7	23.5	29.2	—
$Cr(CO)_5$(iso-$C_2H_2Cl_2$)	2.292 (CH_2), 2.365 (CCl_2)	1.388	172.7	—	30.7	—
$Cr(CO)_5$(*cis*-$C_2H_2Cl_2$)	2.337	1.389	172.1	—	30.4	—
$Cr(CO)_5$(*trans*-$C_2H_2Cl_2$)	2.272	1.392	170.9	27.5	—	43.0
$Cr(CO)_5(C_2HCl_3)$	2.278 (CHCl) 2.309 (CCl_2)	1.404	170.5	—	31.8	41.9
$Cr(CO)_5(C_2Cl_4)$	2.291	1.424	169.8	—	—	38.8
$Mo(CO)_5(C_2H_4)$	2.497	1.377	173.9	17.1	—	—
$Mo(CO)_5(C_2H_3Cl)$	2.473 (CH_2), 2.507 (CHCl)	1.376	172.8	19.8	24.8	—
$Mo(CO)_5$(iso-$C_2H_2Cl_2$)	2.452 (CH_2), 2.533 (CCl_2)	1.381	172.5	—	26.6	—
$Mo(CO)_5$(*cis*-$C_2H_2Cl_2$)	2.498	1.383	172.9	—	26.1	—
$Mo(CO)_5$(*trans*-$C_2H_2Cl_2$)	2.430	1.387	171.8	24.2	—	38.7
$Mo(CO)_5(C_2HCl_3)$	2.429 (CHCl), 2.464 (CCl_2)	1.399	171.4	—	28.9	38.3
$Mo(CO)_5(C_2Cl_4)$	2.436	1.419	170.4	—	—	36.3
$W(CO)_5(C_2H_4)$	2.505	1.378	171.8	17.4	—	—
$W(CO)_5(C_2H_3Cl)$	2.481 (CH_2), 2.512 (CHCl)	1.377	171.6	20.6	25.1	—
$W(CO)_5$(iso-$C_2H_2Cl_2$)	2.458 (CH_2), 2.528 (CCl_2)	1.384	170.7	—	27.5	—
$W(CO)_5$(*cis*-$C_2H_2Cl_2$)	2.495	1.385	171.1	—	27.1	—
$W(CO)_5$(*trans*-$C_2H_2Cl_2$)	2.431	1.390	170.8	26.0	—	39.3
$W(CO)_5(C_2HCl_3)$	2.429 (CHCl) (CCl_2)	1.402	170.1	—	30.2	39.2
$W(CO)_5(C_2Cl_4)$	2.436	1.422	169.5	—	—	37.0

[a] Bond lengths in angstroms, angles in degrees. [b] Pyramidalization angle = 180 − dihedral angle.

TABLE 3: Calculated Bond Dissociation Energies (ΔE) and Enthalpies (ΔH) for $M(CO)_5(C_2Cl_nH_{4-n})$ (n = 0−4; M = Cr, Mo, and W) Complexes (All Values Are in kcal/mol)

	Cr		Mo		W	
olefin	ΔE	ΔH	ΔE	ΔH	ΔE	ΔH
C_2H_4	23.16	21.21	23.54	22.63	25.89	26.16
C_2ClH_3	17.72	18.20	18.45	19.32	21.10	21.62
iso-$C_2Cl_2H_2$	12.45	19.56	13.45	19.90	16.38	24.02
cis-$C_2Cl_2H_2$	13.46	14.11	14.44	15.40	17.43	18.69
trans-$C_2Cl_2H_2$	13.56	15.31	14.29	14.01	17.34	19.81
C_2Cl_3H	8.63	15.92	9.74	16.03	13.12	21.39
C_2Cl_4	3.62	12.55	5.10	12.60	8.97	17.79

TABLE 4: Results of the BEDA for for $M(CO)_5(C_2Cl_nH_{4-n})$ (n = 0−4; M = Cr, Mo, and W) Complexes (All Values Are in kcal/mol)

	ΔE_{pauli}	ΔE_{elect}	ΔE_{oi}	ΔE_{reorg} (olefin)	ΔE_{reorg} ($M(CO)_5$)
$Cr(C_2Cl_4)$	−110.15	63.87	74.12	−21.39	−2.93
$Cr(C_2Cl_3H)$	−96.92	58.87	65.56	−16.64	−2.44
Cr(iso-$C_2Cl_2H_2$)	−89.50	56.53	59.14	−12.13	−1.74
Cr(*cis*-$C_2Cl_2H_2$)	−82.18	52.61	54.17	−9.65	−1.64
Cr(*trans*-$C_2Cl_2H_2$)	−101.34	64.20	68.02	−15.30	−2.06
$Cr(C_2ClH_3)$	−83.43	55.85	54.63	−8.11	−1.31
$Cr(C_2H_4)$	−85.60	59.85	54.92	−5.49	−1.03
$Mo(C_2Cl_4)$	−97.22	58.56	63.97	−18.99	−1.54
$Mo(C_2Cl_3H)$	−88.65	55.54	57.68	−14.94	−1.84
Mo(iso-$C_2Cl_2H_2$)	−83.16	54.17	52.54	−10.71	−1.35
Mo(*cis*-$C_2Cl_2H_2$)	−77.4	51.19	48.56	−8.45	−1.18
Mo(*trans*-$C_2Cl_2H_2$)	−88.23	57.94	57.62	−13.09	−1.73
$Mo(C_2ClH_3)$	−75.26	52.54	48.01	−6.83	−0.07
$Mo(C_2H_4)$	−68.03	51.36	43.86	−3.74	0.10
$W(C_2Cl_4)$	−126.86	77.51	82.89	−23.02	−2.72
$W(C_2Cl_3H)$	−117.33	74.74	76.09	−18.98	−2.49
W(iso-$C_2Cl_2H_2$)	−107.88	71.26	68.52	−14.44	−2.23
W(*cis*-$C_2Cl_2H_2$)	−97.82	65.67	62.25	−11.66	−2.05
W(*trans*-$C_2Cl_2H_2$)	−115.12	76.40	73.89	−16.24	−2.47
$W(C_2ClH_3)$	−97.88	68.43	61.02	−9.31	−2.06
$W(C_2H_4)$	−92.37	68.59	56.81	−5.84	−2.00

Figure 2a clearly shows that the energy difference between the HOMO of the olefin and the LUMO of the $M(CO)_5$ fragment is not affected by the presence of chlorine atoms. On the other hand, the subsequent addition of these electron-withdrawing substituents around the double bond lowers the band gap between the LUMO of a given olefin and the HOMO of the metal fragment so that the π interaction between the two molecular orbitals is more favorable. This trend is observed for all three metals and is in agreement with the foundations of the DCD model. The increase of chlorine atoms decreases the extent of orbital overlap as shown in Figure 2b. This can be attributed to the steric constraints imposed by the size of the chlorine atoms. Thus, the strength of the metal−olefin bond is negatively affected by a decrease in the orbital overlap caused by the size of the substituents around the double bond. The changes in electron population in the HOMO and LUMO of the olefin (Figure 2c) reflect the trends observed in both orbital overlaps and energy gaps described above. It is evident that there is a greater transfer of electron density as the number of chlorines around the double bond increases, mostly as a result of the π back-bonding interaction. In terms of the σ interaction, the amount of electron density transferred decreases slightly as the number of chlorines increase as a result of the decrease in the orbital overlap imposed by steric contraints. Thus, from a molecular orbital perspective the back-bonding dominates the metal−olefin interaction, in good agreement with the DCD model that predicts that an olefin with more electron-withdrawing power should be more favorable for bonding. The influence of the σ bonding is smaller and seems to have an opposite destabilizing effect as the number of chlorines around the double bond increases.

The molecular orbital analyses allow us to conclude that the olefins with more chlorine substituents are much better π bonders, although they are slightly worse as σ bonders. It also tells us that the metal−olefin interaction is dominated by the π interaction and thus an olefin would bond stronger to $M(CO)_5$ in direct proportion to the number of electron-withdrawing atoms. However, the experimental and calculated M−olefin bond enthalpies show a trend opposite to the expected trend from this molecular orbital perspective (in which the DCD model is based). How can then we explain such a contradiction?

Bond Energy Decomposition Analysis of the Metal−Olefin Interaction: Extending the Scope of the DCD Model. Metal−olefin bond energy decomposition analyses provide an answer to the contradiction between the experimental bond

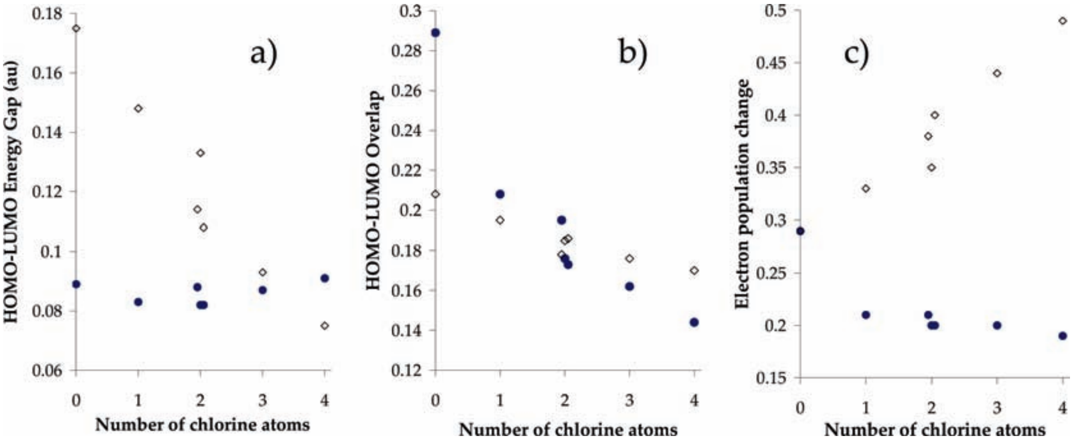

Figure 2. Plots showing the dependence of (a) HOMO−LUMO energy gap, (b) HOMO−LUMO overlap, and (c) the change in the electron population of the HOMO and LUMO of the olefin as a function of the number of chlorines in the olefin. Open symbols denote MOs involved in π back-bonding interactions, and closed symbols denote orbitals involved in σ interactions. For clarity, the values of the disubstituted olefins are shifted slightly so that from left to right they appear in the order, iso-$C_2Cl_2H_2$, *cis*-$C_2Cl_2H_2$, *trans*-$C_2Cl_2H_2$.

energies and the expectation based on a MO analysis and the DCD model. Recall that bond dissociation energies may be split into four terms according to eq 4. Noticeable trends are evident, for instance both the attractive terms $\Delta E_{\mathrm{elect}}$ and ΔE_{oi} increase with an increase in the number of chlorines. ΔE_{oi}, which only accounts for the covalent orbital interactions, follows the trend predicted by the MO analyses and the DCD model. As expected, the magnitude of the repulsive term $\Delta E_{\mathrm{Pauli}}$ also increases with an increase in the number of chlorine atoms. If the magnitude of the sum of the attractive contributions ($\Delta E_{\mathrm{elect}} + \Delta E_{\mathrm{oi}}$) is compared to the magnitude of the repulsive contribution ($\Delta E_{\mathrm{Pauli}}$), we see that the attractive terms dominate the total interaction to a greater degree when there is a smaller number of chlorines around the C═C double bond. This makes sense in terms of steric interactions, because as the number of chlorines decreases, the percentage contribution of the repulsive steric term decreases as well. When the two attractive terms are examined individually it is found that the orbital interaction and electrostatic interaction terms are very close in importance. Qualitatively, when the number of chlorines around the double bond is high, the covalent orbital interaction (ΔE_{oi}) is the dominant term (51−54% of the attractive contribution for C_2Cl_4), but when the number of chlorines is decreased, the electrostatic interaction becomes the dominant term with only 45−49% of the attractive interaction due to covalent orbital interactions. The sum of the first three terms in this equation is the interaction energy (ΔE_{int}), which accounts for the net bonding energy between two reactants in a conformation that corresponds to the geometry they have in the complex. The reorganizational energy ($\Delta E_{\mathrm{reorg}}$) accounts for the energetic cost of the geometrical changes that occur in the $M(CO)_5$ fragment ($\Delta E_{\mathrm{reorg}}(M(CO)_5)$) and the olefin ($\Delta E_{\mathrm{reorg}}$(olefin)) as they interact to form the complex.

In general, ΔE_{int} is not influenced much by the number of chlorine atoms, being about 30−35 kcal/mol. Interestingly, the magnitudes of the attractive (covalent and electrostatic) and repulsive terms seem to increase as more chlorine atoms are added to the olefin at about the same rate. This causes the trend in the total interaction energy to be rather flat. On the other hand, the reorganizational energy depends on the amount of chlorines, with a tendency to increase as the number of halogens increases. Given that the bond dissociation energy is obtained by the combination of the interaction energy and the reorganizational energy, it can be concluded that the bond dissociation energy is definitively influenced by the magnitude of the reorganizational energy.

Interestingly, there are some small differences in the metal complexes of dicholoroethylene isomers. For instance, the BEDA analyses indicate that *trans*-dichloroethylene is the one that interacts the most with the metal, followed by the iso and cis isomers as reflected from the electrostatic ($\Delta E_{\mathrm{elect}}$) and orbital interaction (ΔE_{oi}) energies. This order is also congruent with the MO analysis which indicates that the trans isomer back-bonds better with a given metal because it has a smaller energy gap and better orbital overlap. The three isomers contribute similarly into the σ interaction. The stronger attractive interaction of the trans isomer draws it closer to the metal (bond length is shorter for this isomer) which also accounts for a larger Pauli (steric) orbital repulsion. As discussed previously, the reorganization of the olefin as a consequence of the bonding interaction counts against the total bonding energy, and therefore the trans isomer ends up binding with an energy similar to that of the other two isomers.

Table 4 also shows that the geometrical changes in the olefin accounts for 75−85% of the total reorganizational energy; thus, we can conclude that the conformational changes that occur in the olefin are mostly responsible for the trend seen for the bond dissociation energy. The main geometrical changes occurring are related to the change in orbital hybridization as a result of the metal−olefin σ and π interactions and are manifested in the elongation of the C═C bond and the pyramidalization angle (see Table 2). Figure 3 clearly shows a correlation between these geometrical parameters and the number of chlorine atoms.

The changes that occur in the geometry of the olefin correlate very well to the changes that are observed in reorganizational energy. As more chorines are added, the C═C bond lengthens mostly because of the increase in the electron population of the π^* orbitals in the olefin from the back-bonding interaction with the metal. It is also evident that the change in the pyramidalization angle is increasing as the number of chlorines around the double bond increases. This is a result of a greater change in hybridization of the olefinic carbons toward a more sp^3 like molecular orbital induced by the changes in electron population.

What do these results tell us about the DCD model and its validity? They validate what Cedeño and Weitz had previously implied.[10] The DCD model is purely based on covalent orbital interaction and may be utilized to predict qualitative metal−olefin

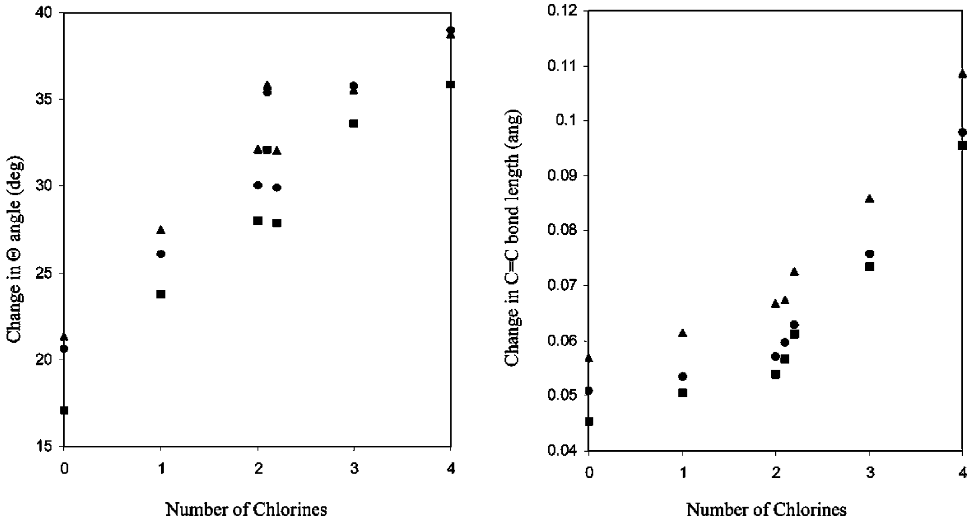

Figure 3. Left: Plot showing the dependence of the change in the pyramidalization angle on the number of chlorines around the double bond. When there is more than one pyramidalization angle in a molecule, the average value is used. Right: Plot showing the dependence of the change of C=C double bond length on the number of chlorines around the C=C double bond. Circles for M = Cr, squares for M = Mo, and triangles for M = W. For clarity, the values of the disubstituted olefins are shifted slightly so that from left to right they appear in the order, *cis*-$C_2Cl_2H_2$, *trans*-$C_2Cl_2H_2$, iso-$C_2Cl_2H_2$.

bonding properties as long as such interaction does not involve energetically expensive reorganization. Our results validate the qualitative predictions of the DCD model. An increase in the electron-withdrawing ability of the olefin increases the extent of back-bonding which in turns increases the attractive covalent and electrostatic interaction energy. However, the available experimental data and the theoretical decomposition analyses make it clear that the attractive orbital interactions (σ and π), which are central to the DCD model, are only one component of the complex interaction between an olefin and a metal. Thus, the prediction of metal−olefin bond strengths and interactions requires a model that rationalizes the contribution of all components in a quantitative manner. For instance, this study shows that even though attractive orbital interactions between $M(CO)_5$ (for M = Cr, Mo, W) and the olefin increase as the olefin becomes more electron withdrawing, this bond-favoring trend is counterbalanced by the Pauli (steric) repulsion energy, which also increases as the number of electron-withdrawing substituents increases. Furthermore, reorganizational energies, which inherently originate from the metal−olefin bonding interaction, play a determining role in the measurable bond strength. As shown in this and previous studies, the magnitude of the reorganizational energy may offset much of the energy gained by attractive metal−olefin interactions.

Conclusions

We have measured and calculated metal−olefin bond energies for the series $M(CO)_5(C_2H_{4-n}Cl_n)$, M = Cr, Mo, and W. The trend in experimental and calculated bond dissociation energies was found to be opposite to the trend expected from general qualitative interpretations of the DCD model. A qualitative interpretation of the DCD model implies that the metal−olefin bond energy should increase in proportion to the electron-withdrawing ability of the olefin which increases with an increase in the number of chlorines around the double bond. Bond energy decomposition analyses demonstrate that if orbital interactions were the unique contributor to the stability of a metal−olefin bond, then bond dissociation energies would follow the trend expected from the DCD model. However, both our experimental measurements and DFT calculations indicate that this is not the case in the complexes studied here. Attractive electrostatic and covalent (orbital) interactions are actually offset by the Pauli (steric) repulsion between the occupied orbitals of the reactants in such a way that the total interaction energy is almost independent of the number of chlorines around the double bond. This study also indicates that the conformational changes in the olefin resulting from stronger covalent bonding interactions increase with the number of chlorine atoms in the olefin. However, these conformational changes have an energetic cost (in terms of reorganizational energy) that has a strong impact on the bond energy. In other words, the reorganizational energy offsets much of the available attractive metal−olefin interaction energy. In summary, an increase in the electron-withdrawing ability of the olefin increases the strength of the attractive covalent interaction as predicted correctly by the DCD model; however, both steric interactions and reorganizational energies also increase in detriment to the overall metal−olefin bond strength. Since these two factors are not included in the DCD model, their inclusion and rationalization should lead us to formulate an extended DCD model that would allow us to predict metal−olefin bond strengths and interactions in a quantitative manner.

Acknowledgment. The authors acknowledge the Petroleum Research Fund, administered by the American Chemical Society (grant no. 39604-GB3), for financial support.

Supporting Information Available: Additional information. This material is available free of charge via the Internet at http://pubs.acs.org.

References and Notes

(1) *Metal-catalysis in Industrial Organic Processes*; Chiusoli, G. P., Maitlis, P. M., Eds.; RSC Publishing: London, 2008.

(2) Crabtree, R. H. *The Organometallic Chemistry of Transition Metals*, 4th ed.; Wiley: New York, 2005.

(3) Bhaduri, S.; Mukesh, D. *Homogeneous Catalysis: Mechanisms and Industrial Applications*; Wiley: New York, 2000.

(4) Parshall, G. W.; Ittel, S. D. *Homogeneous Catalysis: The Applications and Chemistry of Catalysis by Soluble Transition Metal Complexes*, 2nd ed.; Wiley: New York, 1992.

(5) Elschenbroich, C., Salzer, A., *Organometallics: A Concise Introduction*, 2nd ed.; VCH: Weinheim, 1992.

(6) Collman, J. P.; Hegedus, L. S.; Norton, J. R.; Finke, R. G. *Principles and Applications of Organotransition Metal Chemistry*, University Science Books: Mill Valley, CA, 1987.

(7) Dewar, M. J. S. *Bull. Chem. Soc. Fr.* **1951**, *18*, C71.

(8) Chatt, J.; Duncanson, L. A. *J. Chem. Soc.* **1953**, 2939.

(9) Pruchnik, F. P. *Organometallic Chemistry of the Transition Elements*; Plenum Press: New York, NY, 1990; p 343.

(10) Cedeño, D. L.; Weitz, E. *J. Am. Chem. Soc.* **2001**, *123*, 12857.

(11) Tolman, C. A. *J. Am. Chem. Soc.* **1974**, *96*, 2780.

(12) Schlappi, D. N.; Cedeño, D. L. *J. Phys. Chem. A* **2003**, *107*, 8763.

(13) *Computational Organometallic Chemistry*; Cundari, T. R., Ed., Marcel Dekker: New York, 2001.

(14) Laird, B. B.; Ross, R. B.; Ziegler, T. In *Chemical Applications of Density Functional Theory*; ACS Symposium Series 629, Laird, B. B., Ross, R. B., Ziegler, T., Eds.; American Chemical Society: Washington, DC, 1996.

(15) Ziegler, T. *Can. J. Chem.* **1995**, *73*, 743.

(16) Labanowsky, J. K., Andzelm, J. W., Eds. *Density Functional Methods in Chemistry*; Springer-Verlag: New York, 1991.

(17) Ziegler, T. *Chem. Rev.* **1991**, *91*, 651.

(18) Rothberg, L. J.; Simon, J. D.; Bernstein, M.; Peters, K. S. *J. Am. Chem. Soc.* **1983**, *105*, 3464–3468.

(19) Braslavsky, E.; Heibel, G. E. *Chem. Rev.* **1992**, *92*, 1381.

(20) Sound Analysis, version 1.50D; Quantum Northwest, Spokane, WA, 1999.

(21) ADF2004.01 and ADF2008.01; SCM, Theoretical Chemistry, Vrije Universiteit, Amsterdam, The Netherlands;http://www.scm.com.

(22) Becke, A. D. *Phys. Rev. A* **1988**, *38*, 3098.

(23) Perdew, J. P. *Phys. Rev. B* **1986**, *33*, 8822.

(24) Perdew, J. P. *Phys. Rev. B* **1986**, *34*, 7406.

(25) Vosko, S. H.; Wilk, L.; Nusair, M. *Can. J. Phys.* **1980**, *58*, 1200.

(26) van Lenthe, E.; Baerends, E. J.; Snijders, J. G. *J. Chem. Phys.* **1993**, *99*, 4597.

(27) van Lenthe, E.; Baerends, E. J.; Snijders, J. G. *J. Chem. Phys.* **1994**, *101*, 9783.

(28) van Lenthe, E.; Ehlers, A. E.; Baerends, E. J. *J. Chem. Phys.* **1999**, *110*, 8943.

(29) Jaguar 4.1; Schrödinger Inc., Portland, OR, 1991−2000.

(30) Hay, P. J.; Wadt, W. R. *J. Chem. Phys.* **1985**, *82*, 299.

(31) Krishnan, R.; Binkley, J. S.; Seeger, R.; Pople, J. A. *J. Chem. Phys.* **1980**, *72*, 750.

(32) McLean, A. D.; Chandler, G. S. *J. Chem. Phys.* **1980**, *72*, 5639.

(33) Clark, T.; Chandraskhar, J.; Spitznagel, G. W.; Schleyer, P. v. R. *J. Comput. Chem.* **1983**, *4*, 294.

(34) Frisch, M. J.; Pople, J. A.; Binkley, J. S. *J. Chem. Phys.* **1984**, *80*, 3265.

(35) Ziegler, T.; Rauk, A. *Inorg. Chem.* **1979**, *18*, 1755.

(36) Bickelhaupt, F. M.; Baerends, E. J. In *Reviews in Computational Chemistry*; Lipkowitz, K. B., Boyd, D. B., Eds.; Wiley: New York, 2000; Vol. 15.

(37) Morse, J. M., Jr.; Parker, G. H.; Burkey, T. J. *Organometallics* **1989**, *8*, 2471.

(38) Yang, G. K.; Peters, K. S.; Vaida, V. *Chem. Phys. Lett.* **1986**, *125*, 566.

(39) Jiao, T.; Leu, G. L.; Farrell, G. J.; Burkey, T. J. *J. Am. Chem. Soc.* **2001**, *123*, 4960.

(40) Klassen, J. K.; Selke, M.; Sorensen, A. A.; Yang, G. K. *J. Am. Chem. Soc.* **1990**, *112*, 1267.

(41) Klassen, J. K.; Yang, G. K. *Organometallics* **1990**, *9*, 874.

(42) Small, J. R.; Libertini, L. J.; Small, E. W. *Biophys. Chem.* **1992**, *42*, 29.

(43) Brown, C. E.; Ishikawa, Y.-I.; Hackett, P. A.; Rayner, D. M. *J. Am. Chem. Soc.* **1990**, *112*, 2530.

(44) Cedeño, D. L.; Weitz, E. *J. Phys. Chem. A* **2002**, *106*, 4651.

(45) Cedeño, D. L.; Weitz, E.; Bérces, A. *J. Phys. Chem. A* **2001**, *105*, 8077.

(46) Sniatynsky, R.; Cedeño, D. L. *J. Mol. Struct. (THEOCHEM)* **2004**, *711*, 123.

JP9027468